energies

Article

Thermogravimetric, Devolatilization Rate, and Differential Scanning Calorimetry Analyses of Biomass of Tropical Plantation Species of Costa Rica Torrefied at Different Temperatures and Times

Johanna Gaitán-Álvarez [1], Róger Moya [1,*], Allen Puente-Urbina [2] and Ana Rodriguez-Zúñiga [1]

1 Escuela de Ingeniería Forestal, Instituto Tecnológico de Costa Rica, Apartado 159-7050, Cartago, Costa Rica; jgaitan@itcr.ac.cr (J.G.-Á.); ana.rodriguez@itcr.ac.cr (A.R-Z.)

2 Instituto Tecnológico de Costa Rica, Centro de Investigación y de Servicios Químicos y Microbiológicos (CEQUIATEC), Escuela de Quimica, Apartado, 159-7050 Cartago, Costa Rica; apuente@itcr.ac.cr

* Correspondence: rmoya@itcr.ac.cr; Tel.: +506-2550-9092

Received: 18 February 2018; Accepted: 19 March 2018; Published: 21 March 2018

Abstract: We evaluated the thermogravimetric and devolatilization rates of hemicellulose and cellulose, and the calorimetric behavior of the torrefied biomass, of five tropical woody species (*Cupressus lusitanica*, *Dipteryx panamensis*, *Gmelina arborea*, *Tectona grandis* and *Vochysia ferruginea*), at three temperatures (T_T) and three torrefaction times (t_T) using a thermogravimetric analyzer. Through a multivariate analysis of principal components (MAPC), the most appropriate torrefaction conditions for the different types of woody biomass were identified. The thermogravimetric analysis-derivative thermogravimetry (TGA-DTG) analysis showed that a higher percentage of the hemicellulose component of the biomass degrades, followed by cellulose, so that the hemicellulose energy of activation (Ea) was less than that of cellulose. With an increase in T_T and t_T, the Ea for hemicellulose decreased but increased for cellulose. The calorimetric analyses showed that hemicellulose is the least stable component in the torrefied biomass under severe torrefaction conditions, and cellulose is more thermally stable in torrefied biomass. From the MAPC results, the best torrefaction conditions for calorimetric analyses were at 200 and 225 °C after 8, 10, and 12 min, for light and middle torrefaction, respectively, for the five woody species.

Keywords: thermogravimetric analysis; differential scanning calorimetry; hemicellulose; cellulose; torrefaction; thermostability

1. Introduction

Biomass is widely available worldwide, and often used in biofuel production to help reduce the use of fossil energy reserves and mitigate problems the environmental problems caused by petroleum derived fuels [1]. In addition, biomass produces lower carbon dioxide (CO_2) emissions, as it maintains the carbon cycle by freeing the carbon that was previously fixed during photosynthesis [2]. However, despite the importance of biomass, it has not been developed into other types of energy, such as hydroelectricity, eolic, or solar energies, which are being highly exploited [3].

Despite the increase in the use of biomass as an energy source, some disadvantages still limit its optimum performance, such as difficulties in collection due to disperse distribution, irregular shape, high volume, low energy density, and storage and transportation problems [2]. These problems affect the variability of the biomass's physical properties [4]. Other challenges posed by biomass include its low calorific power, high moisture content, and hygroscopic nature that cause economic problems and deficiencies during transportation, handling, storage, and conversion of the material [5].

Technologies that use thermal treatment of biomass could be applied to solve the mentioned difficulties and convert biomass into energy via combustion [6]. Of the thermal treatments, torrefaction appears to be an effective solution [5]. Studies have shown that torrefaction increases the energy density of the biomass and reduces its hygroscopicity [7,8]. Biomass torrefaction occurs at temperatures from 200 and 300 °C, at atmospheric pressure, and in the presence of inert atmosphere, meaning a limited oxygen presence during the process. The advantages of torrefaction include calorific power increase, reduction of O-H and H-C, lower, moisture content, higher hydrophobicity, and better grinding capacity [9–12].

The success and quality of the torrefied biomass depend on the temperature and time of torrefaction, mainly due to the heterogeneity of the chemical composition of the biomass [13]. Among the chemical components of biomass, lignin is the most thermally stable, followed by cellulose and then by [5,12,14]. For average ranges of torrefaction, the component that degrades the most is hemicellulose as well as some non-structural components, such as extractives [9,12,15].

Important changes in biomass composition were observed using thermogravimetric analysis (TGA) after torrefaction [16]. The curves in this analysis demonstrate the thermal stability of the components of the biomass, including the mass loss and residual mass [14,17]. Previous studies confirmed that hemicellulose decreased and, consequently, the proportion of cellulose and lignin increased in the species after torrefaction [12]. However, the characteristics of the torrefied biomass of tropical species have rarely been studied [12,18]. Large volumes of biomass residues of tropical species in Costa Rica are constantly produced in the timber industry, so torrefaction is an option to process this raw material [12,19]. The biomass of tropical timber species and the different torrefaction processes have been characterized [18–21]. This study continued these studies on the biomass torrefaction of the most used species with energy potential in Costa Rica [22–24].

The present study aimed to evaluate the thermogravimetric behaviour, devolatilization of hemicellulose and cellulose, and the calorimetric behaviour of the torrefied biomass of five tropical woody species (*Cupressus lusitanica*, *Dipteryx panamensis*, *Gmelina arborea*, *Tectona grandis* and *Vochysia ferruginea)*, at three temperature conditions (light, middle and severe) and three torrefaction times using simultaneous thermogravimetric and differential scanning calorimetry analyses. Then, we aimed to find the most appropriate torrefaction conditions for the different types of woody biomass using multivariate analysis of principal components (MAPC) in relation to the thermo-chemical degradation without significantly affecting the chemical composition of the material. This study will enhance the treatment of biomass to obtain renewable and viable raw material for the generation of clean energy from a lignocellulosic material [25].

2. Material and Methods

2.1. Material Characteristics

The woody waste biomass of *C. lusitanica*, *D. panamensis*, *G. arborea*, *T. grandis* and *V. ferruginea* from fast growth plantations at different sites in Costa Rica was used. The age of the plantations ranged between 8 and 14 years. The details of the materials are available in Moya et al. [18] and Gaitán-Álvarez et al. [12,21]. Sawdust from all the species was directly collected from the sawing process, conditioned to a 7% moisture content and then sieved. After sieving, the sawdust particles used were 70% of 2.00–4.00 mm and 30% 0.42–2.00 mm. The chemical compositions of the five species are shown in Table 1.

Table 1. Chemical composition of five fast-growth plantation species in Costa Rica.

Properties	*Cupressus lusitanica*	*Dipterix panamensis*	*Gmelina arborea*	*Tectona grandis*	*Vochysia ferruginea*
Cellulose (%)	64.7	49.9	55.6	54.4	50.9
Lignin (%)	31.4	20.3	24.2	21.90	11.2
Ash (%)	0.18	3.04	0.96	2.81	0.99
Carbon (%)	50.18	48.64	48.39	49.77	49.32
Nitrogen (%)	0.27	0.24	0.20	0.20	0.27

2.2. Torrefaction Process

Three 500 g samples of sawdust were obtained from each species. The material was then divided to apply three different torrefaction durations (8, 10 and 12 min), and the three different torrefaction temperatures (200, 225, and 250 °C), resulting in nine treatments per species. Figure 1 shows the nine treatment and their abbreviations. These durations and temperatures were selected according to a previous study [5]. A modified Thermolyne Furnace 48,000 (Thermolyne, Waltham, MA, USA) was used for the torrefaction process. The furnace was sealed to prevent airflow from the manual system to maintain pressure. Every 4–5 min, the air was freed, allowing the development of the torrefaction process within an environment with limited oxygen content, adding N_2 to the furnace [19].

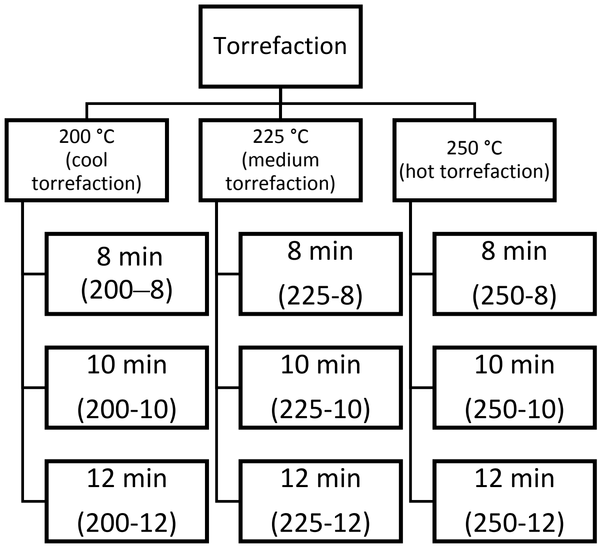

Figure 1. Temperature and time for the torrefaction of the biomass of five fast-growth plantation species of Costa Rica. Note: the numbers in parentheses indicate the abbreviation of this torrefaction condition.

2.3. Thermogravimetric Analysis (TGA)

To obtain the degradation curves, TGA was performed at atmospheric pressure under inert ambient nitrogen, using about 5 mg of sawdust of each species. The heating rate was 20 °C/min in a nitrogen atmosphere of ultra-high purity N_2 at 100 mL/min, reaching a temperature of 800 °C. A TA Instruments (New Castle, DE, USA) thermogravimetric analyzer, model SDT Q600, was used. The TGA provided values for mass loss in relation to temperature, from which the derivative thermogravimetry (DTG) was obtained, allowing us to determine the position and temperature at which sample degradation occurred. The TGA data and their first and second derivatives (DTG and D^2TG) were analyzed using TA Instruments Universal Analysis 2000 software. The parameters are presented in Figure 2a,b: (i) the temperature at the beginning of degradation (T_i) and the percentage of residual mass at Ti (W_{Ti}); (ii) the temperature corresponding to the maximum degradation of hemicellulose (T_{sh}) and the percentage of residual mass at T_{sh} (WT_{sh}); (iii) the temperature corresponding to the maximum cellulose mass loss rate (T_m) and the percentage of the residual mass at Tm (W_{Tm}) and (iv) the temperature corresponding to the end of degradation (T_f) and the percentage of residual mass at T_f (W_{Tf}), when mass loss began to stabilize as the temperature increased. Additional parameters were obtained from the derivative thermogravimetry (DTG): (v) the temperature of hemicellulose degradation onset ($T_{onset(hc)}$) and residual mass at $T_{onset(hc)}$ ($W_{Tonset\ (hc)}$); (vi) the end temperature of the hemicellulose degradation ($T_{offset(hc)}$) and the residual mass at $T_{offset(hc)}$ ($W_{Toffset\ (hc)}$); (vii): the temperature of cellulose degradation onset ($T_{onset(c)}$) and the residual mass at T onset(c) ($W_{Tonset(c)}$); (viii): the end temperature of cellulose degradation ($T_{offset(c)}$)and the residual mass at $T_{offset(c)}$ ($W_{Toffset(c)}$). Figure 2c shows the DTG curve representing the different temperature. MAgicPlot 2.5.1 software was used to obtain these values.

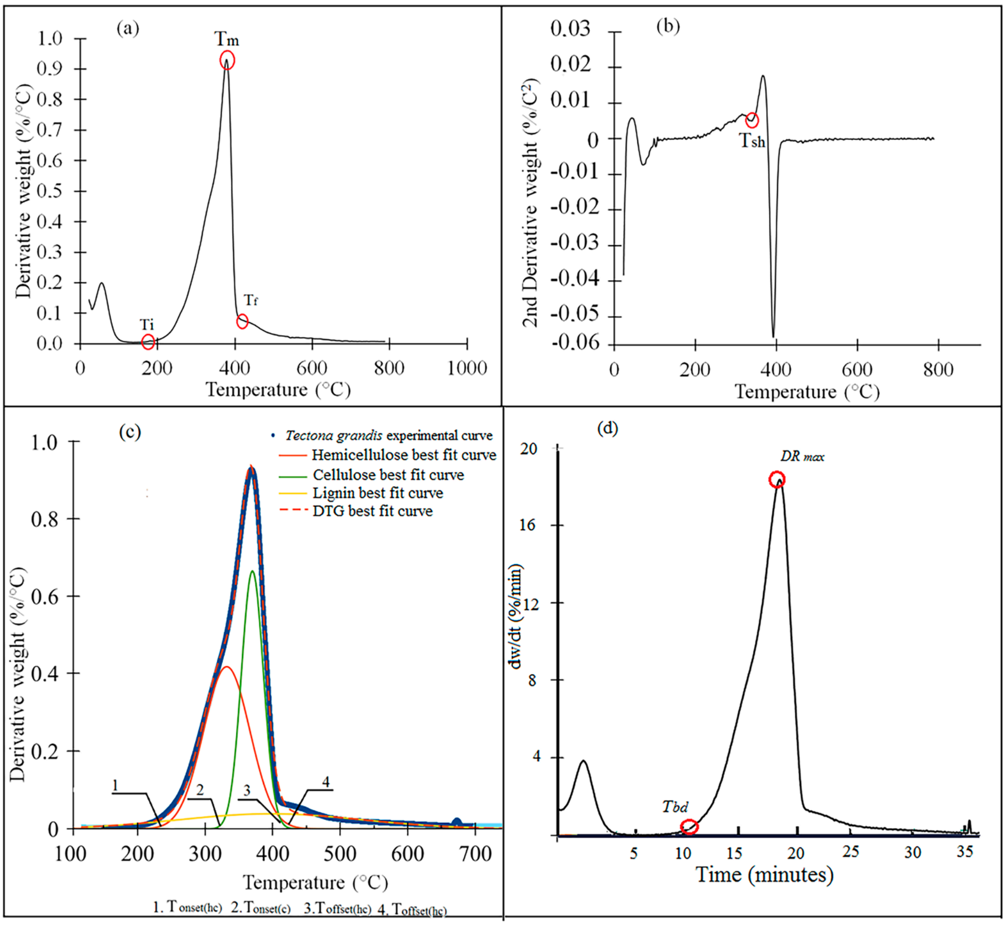

Figure 2. (**a**,**c**) Derivative thermogravimetry (DTG) and (**b**) second derivative (D^2TG) parameters for the different woody biomasses analyzed; (**d**) Devolatilization rate measured by first time derivates of the mass frcationas a function of time. Note: t_{bd} is the start time of the maximum devolatilization rate and D_{max} is the maximum devolatilization rate [18].

Once the decomposition start points for hemicellulose and cellulose were obtained, the thermostability of these components was evaluated using the model described in Equation (2), which was obtained from the linearized model in Equation (1) according to Sbirrazzuoli et al. [26]. The differential was the conversional method used by Friedman. The objective was to calculate the activation energy of the decomposition for each component of the materials being studied (hemicellulose and cellulose):

$$K = A * e^{\left(\frac{-Ea}{RT}\right)} \quad (1)$$

$$\ln\left(\frac{d\alpha}{dt}\right) = \ln K_0 + \left(\frac{-Ea}{RT}\right) + n * \ln(1-\alpha) \quad (2)$$

where α is the degraded mass, $\frac{d\alpha}{dt}$ is the percentage of the degraded sample per unit time, A is the pre-exponential factor, Ea is the energy of activation, and T is temperature.

2.4. Devolatilization Variation

Several methods can be used to measure the degree of biomass devolatilization [18,27]. According to Grønli et al. [27], the total volatiles released during devolatilizatiion include mass fractions, whose dynamics are described by first-order kinetics. In this research, the devolatilization behavior during the thermal degradation of the biomass components in different samples was evidence by the percentage of devolatilized mass relative to time, and a subsequent analysis of the devolatilization rate (D_{rate}). The D_{rate} behavior with different T_T and t_T was first described. Next, we determined the maximum devolatilization rate (D_{max}) and the time at which D_{rate} was obtained. Figure 2d shows where these parameters were determined in the first time derivatives of the mass fraction with respect to time.

2.5. Statistical Analysis

The experiment had a two-level factorial design. Level one corresponded to the t_T of the biomass at three different times: 8, 10, and 12 min. The second factorial level was T_T at three temperatures: 200, 225, and 250 °C. This design was applied to each species studied (*C. lusitanica*, *D. panamenisis*, *G. arborea*, *T. grandis* and *V. ferruginea*). We worked with three samples for each treatment per species. Secondly, a multivariate analysis of the principal components (MAPC) was performed, including all the variables of the TGA and the determined devolatilization parameters. Two main components were selected. This analysis was performed with SAS software (SAS Inc., Cary, NC, USA). Significance level was established at 5%.

3. Results

3.1. TGA-DTG Analysis

The thermogravimetric decomposition behavior of the torrefied biomass for the five species showed the same pattern with different T_T and t_T (Figure 3a–h). However, the DTG curve showed some differences in biomass decomposition (Figure 3a–h). For the TGA curve, five important stages were observed. A predominant signal appeared in the first stage prior to 100 °C. The second stage showed a pronounced peak between 290 °C and 330 °C, the third stage occurred between 340–380 °C. And the fourth stage appeared between 400–500 °C, where the speed of mass loss mas lower compared with the two previous decomposition stages. Finally, few changes in the sample occurred as temperature continued to increase.

Overall, the TGA and DTG curves (Figure 3a–h) showed small visually noticeable differences in the thermal behaviour of the torrefied biomass at various T_T. For all species studied, the biomass torrefied at 250 °C at the three t_T were thermally different. First, the TGA curves show that the biomass torrefied at 250 °C, or severe torrefaction, behaved differently compared to the rest of the T_T. After 340–380 °C, mass loss was less than for biomass torrefied at 250 °C (Figure 3a–h). Second, the DTG curves showed a strong signal at 290 °C, but it appeared as a small shoulder along that at 250 °C (Figure 3a–h). This signal was more visible in *D. panamensis* (Figure 3c) and *V. ferruginea* (Figure 3i), whereas this shoulder was not present in *C. lusitanica* (Figure 3a), *G. arborea* (Figure 3e), and *T. grandis* (Figure 3g) in biomass torrefied at 250-12.

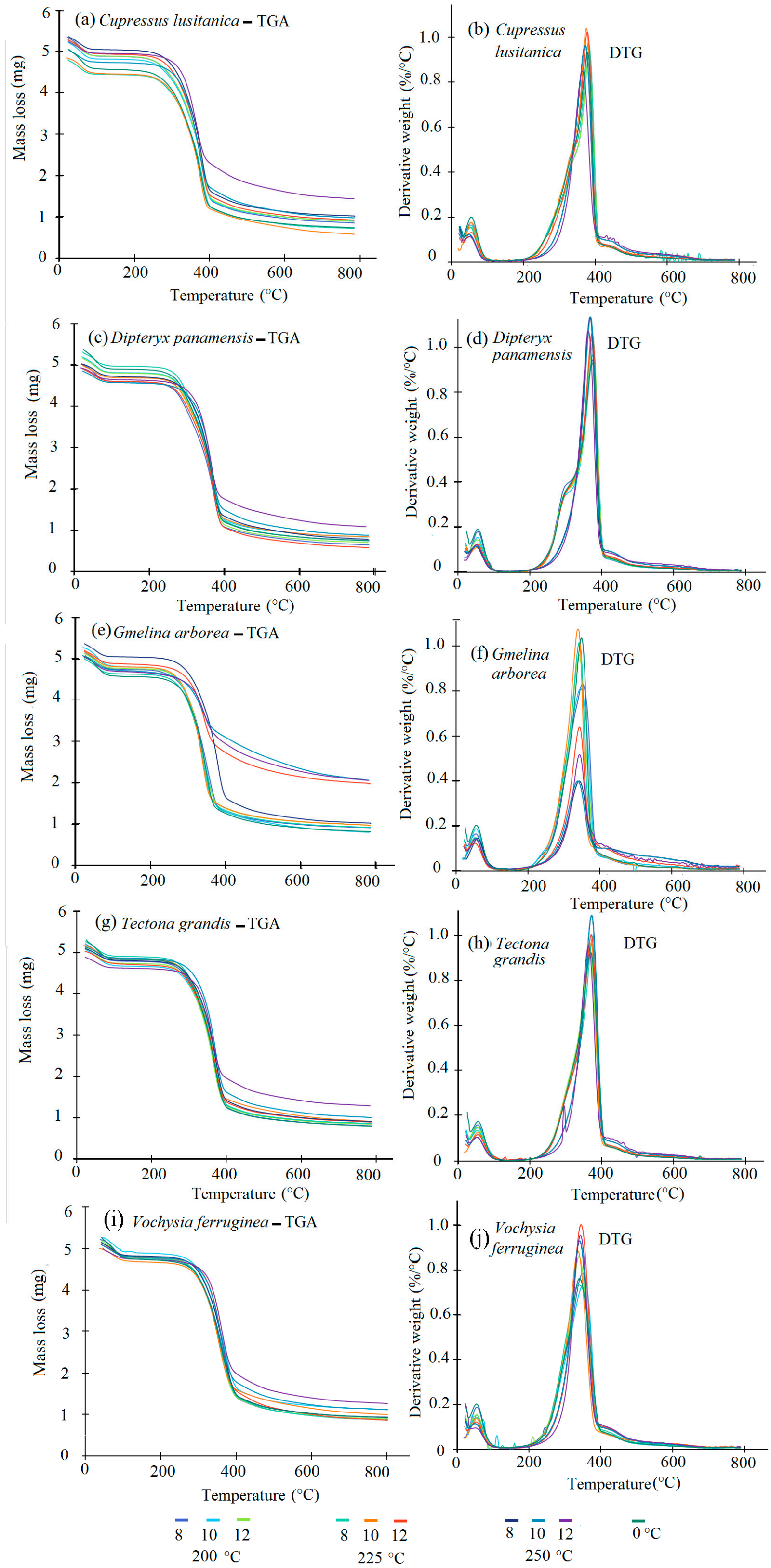

Figure 3. Thermogravimetric analysis (TGA) and DTG of biomasses for *Cupressus lusitanica* (**a**–**b**), *Dipteryx panamensis* (**c**–**d**), *Gmelina arborea* (**e**–**f**) and *Tectona grandis* (**g**–**h**) and *Vochysia guatemalensis* (**i**–**j**), torrefied at different times and temperatures.

Tables 2 and 3 show the detailed analyses of the temperatures and mass loss for the various species, where the main changes in the degradation of the different chemical components of the torrefied biomass during the TGA occurred. In the evaluation of the decomposition T_i in *C. lusitanica*, the T_i of biomass torrefaction increased with respect to untorrefied biomass, except for the 250-8 condition. For the remaining four species under all torrefaction conditions, decomposition T_i increased (Table 2). As for W_{Ti} at 250 °C, torrefaction was greater in the torrefied biomass compared with untorrefied biomass for all species (Table 3). Conversely, T_i tended to increase in torrefied biomass under the light torrefaction condition (200-8) to the middle torrefaction condition between 225-10 and 225-12, depending on the species, and decreased under 250-10 or 250-12 conditions. For *D. panamensis*, *G. arborea*, *T. grandis*, and *V. ferruginea*, the decomposition T_f was lower for the torrefied biomass than the untorrefied biomass under any condition of T_T and t_T. T_f increased at 200 °C in the torrefied biomass of *C. lusitanica* compared to untorrefied biomass. The remaining conditions (225 and 250 °C) displayed lower T_f compared to the untorrefied biomass (Table 2). The behavior of W_{Ti}, W_{Tf}, and the residual mass differed among T_i and T_f conditions for all species, as W_{Ti} and W_{Tf} increased with increasing T_T and t_T (Tables 2 and 3).

C. lusitanica behaved differently with respect to hemicellulose parameters compared with the other species. $T_{onset(hc)}$ and T_{sh} were higher in the torrefied biomass compared to the untorrefied biomass (Table 2), whereas the $T_{offset(hc)}$ was lower in all torrefied biomasses compared to the untorrefied biomass (Table 2). $T_{onset(hc)}$ was lower in the torrefied biomass of *D. panamensis*, *G. arborea*, *T. grandis*, and *V. ferruginea* compared to untorrefied biomass. The T_{sh} and $T_{offset(hc)}$ of the torrefied biomass of these species were higher than the untorrefied biomass (Table 2).

The different torrefaction conditions had varying effects on the hemicellulose of *C. lusitanica* compared to the other four species. The $T_{onset(hc)}$ of the torrefied biomass of *C. lusitanica* increased as T_T and t_T increased, whereas T_{sh} and $T_{offset(hc)}$ decreased with increasing T_T and t_T. The $T_{onset(hc)}$ also increased in the torrefied biomass of the remaining species (*D. panemensis*, *G. arborea*, *T. grandis* and *V. feruginea*) under light 200-8) to medium (between 225-10 or 225-12 depending on the species), torrefaction conditions, then decreasing under the 250-10 or 250-12 conditions. For the T_{sh} and $T_{offset(hc)}$ parameters, their values decreased with increasing T_T and t_T, whereas some irregularities were observed in this behaviour in *C. lusitanica* and *T. grandis.*

In biomass torrefied at any T_T or t_T, $W_{Tonset(hc)}$, W_{Tsh}, and $W_{Toffset(hc)}$ had higher values than in untorrefied biomass in all species (Table 3). The values of T_T and t_T varied under different torrefaction conditions. In general, the values of $W_{Tonset(hc)}$, W_{Tsh} and $W_{Toffset(hc)}$ for all species increased with increasing T_T, particularly in biomass torrefied at 250 °C. Few changes were observed in t_T at the same T_T in the $W_{Tonset(hc)}$ and W_{Tsh} values for all t_T of the different species. However, for $W_{Toffset(hc)}$, for 8 and 10 min, the parameter values were similar, whereas under condition 250-12, a significant increase in $W_{Toffset(hc)}$ was observed in all species (Table 3).

For the cellulose decomposition parameters, biomass torrefaction increased $T_{onset(c)}$ compared to the untorrefied biomass in *C. lusitanica*, *G. arborea*, *T. grandis,* and *V. ferruginea*, whereas in *D. panamensis*, $T_{onset(c)}$ increased from the 200-8 to the 250-10 condition, and then decreased under the most severe condition (250-12) (Table 3). Conversely, T_m increased in the torrefaction of the biomass of *C. lusitanica* and *D. panamensis* from the least severe condition (200-8) to condition 225-10. Also, under conditions 225-12 and T_T at 250 °C, the torrefied biomass had a lower T_m than the untorrefied biomass. The torrefied biomass of *G. arborea* had a higher T_m value compared to the untorrefied biomass, except under condition 250-8. In the biomass of *T. grandis*, torrefaction increased T_m compared to untorrefied biomass, except for condition 250-12. In the biomass of *V. ferruginea*, torrefaction reduced T_m under conditions 200-12, 225-8, and 225-10, whereas T_m was higher under the rest of the torrefaction conditions (Table 3) compared with untorrefied biomass. Lastly, torrefaction of the biomass of the five species decreased $T_{offset(c)}$ compared with untorrefied biomass (Table 3).

Table 2. Thermogravimetric analysis (TGA) temperatures of biomasses of five fast-growth plantation species in Costa Rica torrefied at different times and temperatures.

Species	Temperature (°C)	Time (min)	T_i (°C)	T_f (°C)	Residual Mass (%)	$T_{onset(hc)}$ (°C)	$T_{offset(hc)}$ (°C)	T_{sh} (°C)	$T_{onset(c)}$ (°C)	$T_{offset(c)}$ (°C)	T_m (°C)
Cupressus lusitanica	0	0	172.1	448.7	21.0	221.2	455.4	339.3	253.8	465.8	378.8
	200	8	177.2	449.8	22.6	231.2	454.4	345.3	345.5	418.7	383.5
		10	181.7	438.0	24.1	234.0	452.3	340.1	346.4	418.1	383.5
		12	191.7	453.5	23.3	231.4	454.5	345.3	346.1	418.4	382.6
	225	8	215.4	436.2	22.8	230.9	452.4	346.5	344.6	416.4	380.8
		10	183.5	412.6	23.6	237.1	438.2	329.7	340.1	409.7	375.3
		12	173.5	445.3	25.0	245.0	439.1	337.5	341.2	413.6	378.0
	250	8	161.7	437.1	28.3	247.9	440.9	342.7	343.4	415.7	379.8
		10	172.6	425.3	31.3	266.5	425.7	263.5	333.5	413.8	371.7
		12	213.8	476.6	36.1	273.5	415.8	275.2	323.3	410.7	364.4
Dipteryx panamensis	0	0	146.3	460.9	18.7	239.5	375.4	315.0	238.2	468.2	372.1
	200	8	194.7	431.1	19.6	206.9	438.6	310.2	330.3	413.0	373.8
		10	188.2	441.3	21.5	206.4	443.0	307.6	330.4	416.7	375.1
		12	201.2	425.7	20.2	205.2	443.1	306.3	332.4	415.6	375.1
	225	8	212.8	430.9	20.8	211.6	440.9	316.7	333.0	411.3	373.8
		10	205.1	433.5	23.4	211.0	437.9	314.1	331.2	409.2	372.5
		12	206.4	446.5	18.5	212.4	441.3	311.5	331.2	411.9	372.5
	250	8	212.8	433.5	24.1	237.6	428.4	308.9	325.7	409.3	367.3
		10	206.4	438.7	27.2	263.6	420.2	272.6	329.8	407.9	368.6
		12	196.0	424.4	33.5	266.1	413.8	272.6	232.8	404.0	362.1
Gmelina arborea	0	0	172.1	471.5	20.8	249.1	385.0	305.8	258.7	417.9	349.9
	200	8	194.7	410.2	24.4	196.7	392.7	247.9	305.6	395.6	351.7
		10	197.3	401.1	24.4	225.1	410.4	247.9	301.7	401.6	346.5
		12	221.9	419.2	25.5	217.9	417.2	302.4	295.9	391.7	341.4
	225	8	201.2	399.8	26.6	227.0	411.4	303.7	305.3	381.4	341.4
		10	199.9	406.3	26.4	236.3	391.9	240.1	303.9	376.0	338.8
		12	207.7	424.4	50.0	238.5	418.1	262.2	305.2	380.7	344.0
	250	8	173.9	454.3	25.8	247.9	440.9	267.4	343.4	415.7	341.4
		10	198.6	442.6	56.9	236.6	416.5	242.7	295.0	384.6	337.5
		12	179.1	412.8	56.9	188.0	495.9	255.7	294.7	386.6	344.0

Table 2. *Cont.*

Species	Temperature (°C)	Time (min)	T_i (°C)	T_f (°C)	Residual Mass (%)	$T_{onset(hc)}$ (°C)	$T_{offset(hc)}$ (°C)	T_{sh} (°C)	$T_{onset(c)}$ (°C)	$T_{offset(c)}$ (°C)	T_m (°C)
Tectona grandis	0	0	164.5	473.0	19.2	262.6	398.5	321.0	257.8	454.6	368.2
	200	8	233.6	425.7	22.1	226.6	435.2	312.8	322.0	418.8	371.2
		10	219.3	430.9	23.2	233.0	433.8	320.6	330.2	410.6	369.9
		12	227.1	425.7	23.1	225.7	434.4	316.7	320.4	413.4	366.0
	225	8	198.6	438.7	22.1	227.2	441.1	312.8	320.4	413.4	373.8
		10	220.6	423.1	26.5	233.0	430.8	312.8	329.1	409.6	369.9
		12	233.6	443.9	24.2	232.0	434.8	316.7	328.6	411.9	369.9
	250	8	212.8	432.2	25.1	240.2	434.9	308.9	330.8	414.9	373.8
		10	241.4	427.0	28.8	266.0	422.4	286.8	331.9	412.0	369.9
		12	272.6	430.9	36.9	256.6	416.1	298.5	317.6	408.6	363.4
Vochysia ferruginea	0	0	161.5	439.6	22.3	233.7	369.6	301.3	227.2	442.9	339.3
	200	8	219.3	427.0	22.5	220.1	414.8	301.1	301.9	407.7	350.4
		10	233.6	430.9	26.2	222.0	419.1	306.3	306.3	408.1	355.6
		12	223.2	424.4	22.9	217.1	384.1	299.8	282.2	405.5	338.8
	225	8	224.5	420.5	23.7	222.3	415.6	255.7	297.9	408.4	337.5
		10	224.5	401.1	29.6	214.5	407.1	298.5	286.1	394.1	336.2
		12	251.8	432.2	24.8	237.9	401.2	245.3	294.2	400.5	346.5
	250	8	245.3	415.4	24.7	224.4	414.8	297.2	303.4	406.7	350.4
		10	245.1	420.5	30.4	228.4	401.8	253.1	288.4	398.4	340.1
		12	227.1	414.1	35.3	251.7	395.4	268.7	294.8	395.7	342.7

Table 3. TGA residual masses of the biomasses of five fast-growth plantation species in Costa Rica torrefied at different times and temperatures.

Specie	Temperature (°C)	Time (min)	W_{Ti} (%)	W_{Tf} (%)	$W_{Tonset(hc)}$ (%)	$W_{Toffset (hc)}$ (%)	W_{Tsh} (%)	$W_{Tonset(c)}$ (%)	$W_{Toffset(c)}$ (%)	W_{Tm} (%)
Cupressus lusitanica	0	0	90.3	21.0	89.7	20.6	65.4	88.1	20.0	38.5
	200	8	91.2	22.6	90.4	22.3	65.3	65.3	24.7	39.8
		10	91.8	24.1	91.0	23.3	68.5	65.7	25.6	40.5
		12	92.0	23.3	91.3	23.2	66.2	65.7	25.7	41.7
	225	88	92.0	22.8	91.7	21.7	65.1	66.1	24.2	40.9
		10	92.0	23.6	91.1	21.8	71.9	66.5	23.9	40.4
		12	93.3	25.0	92.3	25.5	72.9	71.0	27.5	43.8
	250	8	94.0	28.3	92.8	26.8	72.1	71.6	28.8	42.5
		10	93.7	31.3	92.1	31.3	92.3	79.4	32.5	52.7
		12	94.1	36.1	92.7	42.1	92.6	86.1	42.7	62.2
Dipteryx panamensis	0	0	90.9	18.7	89.6	35.5	72.6	89.7	18.4	38.3
	200	8	91.4	19.6	91.3	19.3	74.0	65.6	20.6	36.5
		10	92.4	21.5	92.3	21.4	78.1	69.4	22.8	39.6
		12	92.6	20.2	92.6	19.2	77.8	67.6	20.8	37.7
	225	8	93.1	20.8	93.1	20.2	21.7	68.4	22.1	39.6
		10	93.8	23.4	93.8	23.2	77.0	70.0	25.0	41.1
		12	93.4	18.5	93.3	18.8	77.4	69.1	20.8	39.5
	250	8	93.4	24.1	92.8	24.4	82.9	76.8	25.9	46.4
		10	93.8	27.2	92.3	28.8	91.7	83.8	30.1	50.9
		12	93.9	33.5	92.3	34.5	92.0	93.4	35.3	56.4
Gmelina arborea	0	0	89.8	20.8	88.0	26.0	76.1	87.2	23.5	44.1
	200	8	91.4	24.4	91.4	25.6	89.2	76.4	25.4	45.9
		10	90.8	24.4	90.0	23.8	88.4	75.7	24.4	46.1
		12	92.3	25.5	92.4	25.6	78.4	81.3	27.5	51.0
	225	8	92.2	26.6	91.7	25.7	77.2	76.3	28.2	49.5
		10	92.5	26.4	91.5	27.5	91.3	76.9	29.1	49.0
		12	93.0	50.0	92.3	50.6	91.1	85.1	54.8	67.5
	250	8	93.9	25.8	92.8	26.8	91.6	71.6	28.8	72.5
		10	92.1	56.9	91.1	59.4	90.9	86.5	62.7	74.4
		12	92.4	56.9	92.3	50.0	90.5	87.5	60.0	72.2

Table 3. *Cont.*

Specie	Temperature (°C)	Time (min)	W_{Ti} (%)	W_{Tf} (%)	$W_{Tonset(hc)}$ (%)	$W_{Toffset (hc)}$ (%)	W_{Tsh} (%)	$W_{Tonset(c)}$ (%)	$W_{Toffset(c)}$ (%)	W_{Tm} (%)
Tectona grandis	0	0	91.0	19.2	88.8	23.9	74.4	89.2	19.9	43.2
	200	8	91.1	22.1	91.3	21.5	78.5	74.5	22.5	41.5
		10	91.5	23.2	91.2	23.0	76.0	71.7	24.5	44.1
		12	91.9	23.1	91.9	22.5	77.1	75.4	23.9	44.2
	225	8	92.7	22.1	92.4	22.0	79.7	76.7	23.7	43.1
		10	93.1	26.5	92.9	26.1	80.4	73.3	27.4	45.2
		12	92.7	24.2	92.7	24.7	79.5	74.7	26.3	46.2
	250	8	93.7	25.1	93.2	25.0	84.3	76.3	26.5	45.5
		10	93.6	28.8	92.6	29.3	91.0	80.6	30.2	52.9
		12	92.6	36.9	93.2	38.3	89.6	86.5	39.1	58.8
Vochysia ferruginea	0	0	89.6	22.3	88.1	32.3	74.9	88.3	22.2	52.1
	200	8	90.2	22.5	90.2	23.4	76.0	76.0	23.9	45.7
		10	90.8	26.2	91.2	26.9	76.1	76.1	27.6	46.0
		12	91.0	22.9	91.2	26.4	76.9	83.2	24.3	52.0
	225	8	91.4	23.7	91.4	24.1	89.3	78.2	24.7	53.6
		10	92.3	29.6	92.6	29.2	79.6	84.0	30.2	54.6
		12	91.7	24.8	92.4	27.7	92.0	85.9	27.9	52.8
	250	8	91.5	24.7	92.5	24.8	81.6	79.3	25.4	48.9
		10	92.2	30.4	92.9	32.1	91.7	87.2	32.4	58.7
		12	93.5	35.3	92.7	37.4	91.8	88.7	37.4	62.4

With respect to the different torrefaction conditions, the increase in T_T and t_T decreased $T_{onset(c)}$ in *C. lusitanica* and *D. panamensis*. Conversely, in *G. arborea*, the increase in T_T and t_T decreased $T_{onset(c)}$, except under condition 225-8. As for *T. grandis* and *V. ferruginea*, no trend was found in $T_{onset(c)}$ with either an increase or decrease of T_T or t_T (Table 3). T_m and $T_{offset(c)}$ decreased in all species as T_T or t_T increased (Table 3).

The evaluation of the residual mass of the different biomasses showed that torrefaction decreased the $W_{Tonset(c)}$ value in *C. lusitanica* and *T. grandis*, whereas in *D. panamensis*, *G. arborea* and *V. ferruginea*, torrefaction decreased the $W_{Tonset(c)}$ value, except under the most severe condition (250-12) (Table 3). Torrefaction increased T_m in all species, except under condition 200-8 for *D. panamensis* and *T. grandis* and conditions 200-8 and 200-10 for *V. ferruginea*, where T_m decreased. Lastly, $W_{Toffset(c)}$ was higher in torrefied biomass than in untorrefied biomass for all species (Table 3). The evaluation of the residual mass under the different torrefaction conditions showed that all parameters related to residual mass ($W_{Tonset(c)}$, W_{Tm}, and $W_{Toffset(c)}$) increased their values with increasing T_T and t_T of torrefaction in all species (Table 3).

Table 4 shows the kinetic parameters of hemicellulose and cellulose decomposition in torrefied biomass observed with TGA. In the torrefied biomass of *C. lusitanica*, the activation energy (Ea) value of hemicellulose increased with the increase in T_T and t_T up to 225 °C; however, in torrefaction at 250 °C for 10 and 12 min, the Ea values were lower. The Ea cellulose values for the biomass of *C. lusitanica* increased with the increase in T_T and t_T, requiring more energy to degrade the cellulose in the biomass. For Ea, the torrefied biomasses at 200 °C and 225-8 had lower values than the untorrefied biomass; then Ea increased with T_T and t_T, decreasing again under the 250-12 condition.

The torrefaction increased the pre-exponential factor (A) and Ea of the hemicellulose in the *D. panamensis* biomass compared to the untorrefied biomass. The A and Ea increased from 200-8 to 225-12, and decreased at 250 °C. For cellulose, the A and Ea in the torrefied biomass decreased with the increase in T_T and t_T, but any torrefaction produced lower values of A and Ea compared to the untorrefied biomass.

The *G. arborea* torrefied biomass had lower A and Ea hemicellulose values than the untorrefied biomass. Torrefaction at 200 °C had high Ea hemicellulose values, whereas the Ea decreased significantly with T_T and t_T above 225 °C. For cellulose, Ea increased as T_T and t_T increased, especially under condition 225-10 (Table 4). The torrefied biomass had higher Ea values compared to untorrefied biomass, except for conditions 200-8 and 200-10. In general, torrefaction Ea increased with increasing T_T and t_T.

With *T. grandis*, the hemicellulose A and Ea increased up to torrefaction condition 225-12, with values greater than those for untorrefied biomass. Beyond these torrefaction conditions, A and Ea decreased in the torrefied biomass at 250 °C, with values lower than found for the untorrefied biomass. For cellulose, Ea was lower for the different types of torrefied biomass, except under condition 250-12. Ea was also lower in torrefied biomass under 225-8, 225-10, and 250-8 conditions. Ea increased with T_T for the other temperatures. However, Ea was greater for all torrefied biomasses, increasing as T_T and t_T increased (Table 4).

The torrefied biomass of *V. ferruginea* had lower Ea values for hemicellulose than the untorrefied biomass. Ea in hemicellulose decreased with decreasing T_T for the different torrefaction conditions, whereas at the same temperature, Ea decreased at 10 and 12 min. For cellulose, the Ea value was lower as T_T, decreased except for conditions 225-10 and 250-12, in which Ea was higher in the torrefied biomass. For the EA value for cellulose for different T_T, Ea increased with T_T, excluding conditions 200-10 and 225-8, which had a low Ea value.

Notably, the correlation coefficients (R^2) for all torrefaction conditions remained close to 0.99, with the exception of the cellulose models for *G. arborea*, which were low.

Table 4. Activation energies and pre-exponential factors for the thermal decomposition of hemicellulose and cellulose observed in biomasses of five fast-growth plantation species in Costa Rica torrefied at different times and temperatures.

Species	Temperature (°C)	Time (min)	Hemicellulose			Cellulose		
			A	Ea	R^2	A	Ea	R^2
Cupressus lusitanica	0	0	2×10^{9}	77.9	0.999	4×10^{19}	158.3	0.955
	200	8	3×10^{9}	78.5	0.995	8×10^{7}	68.2	0.999
		10	4×10^{9}	79.8	0.993	9×10^{7}	68.5	0.999
		12	5×10^{9}	80.8	0.994	5×10^{7}	65.7	0.999
	225	8	2×10^{10}	87.0	0.996	1×10^{9}	81.4	0.999
		10	1×10^{10}	85.1	0.996	3×10^{17}	177.7	0.997
		12	6×10^{9}	84.3	0.998	9×10^{15}	160.3	0.999
	250	8	3×10^{9}	82.1	0.999	1×10^{16}	161.1	0.998
		10	5×10^{8}	76.0	0.998	2×10^{25}	267.6	0.973
		12	6×10^{7}	68.2	0.996	6×10^{19}	201.1	0.999
Dipteryx panamensis	0	0	2×10^{8}	66.3	0.979	2×10^{8}	324.7	0.977
	200	8	2×10^{12}	105.1	0.997	1×10^{12}	113.4	0.997
		10	4×10^{13}	118.2	0.997	3×10^{12}	119.1	0.997
		12	3×10^{13}	117.6	0.997	6×10^{13}	133.8	0.997
	225	8	1×10^{14}	124.5	0.998	7×10^{15}	157.1	0.994
		10	1×10^{14}	123.1	0.998	1×10^{19}	193.4	0.985
		12	1×10^{13}	113.5	0.998	4×10^{16}	164.9	0.991
	250	8	3×10^{10}	89.7	0.999	6×10^{18}	189.2	0.989
		10	4×10^{8}	75.0	0.999	9×10^{21}	227.4	0.982
		12	2×10^{7}	63.5	0.998	2×10^{28}	299.9	0.946
Gmelina arborea	0	0	3×10^{12}	109.6	0.914	9×10^{15}	146.8	0.777
	200	8	7×10^{8}	72.3	0.989	2×10^{9}	77.6	0.993
		10	8×10^{9}	81.8	0.994	2×10^{11}	96.8	0.986
		12	1×10^{11}	94.1	0.999	4×10^{22}	223.1	0.899
	225	8	3×10^{10}	89.1	1.000	4×10^{24}	244.7	0.810
		10	4×10^{10}	90.2	0.999	2×10^{32}	327.9	0.729
		12	6×10^{6}	56.7	0.997	2×10^{29}	298.7	0.760
	250	8	3×10^{8}	73.1	0.997	1×10^{16}	161.1	0.998
		10	1×10^{6}	51.5	0.999	2×10^{12}	112.7.7	0.999
		12	9×10^{2}	24.5	0.998	5×10^{27}	280.2	0.856
Tectona grandis	0	0	2×10^{9}	79.3	0.997	4×10^{22}	143.6	0.991
	200	8	4×10^{11}	100.7	1.000	9×10^{14}	144.9	0.994
		10	3×10^{11}	100.1	1.000	6×10^{16}	167.4	0.990
		12	1×10^{12}	105.5	1.000	5×10^{19}	198.6	0.971
	225	8	3×10^{12}	109.4	0.999	4×10^{12}	118.9	0.996
		10	2×10^{12}	108.0	0.999	7×10^{12}	121.4	0.994
		12	2×10^{12}	108.5	0.999	4×10^{15}	153.0	0.993
	250	8	4×10^{11}	101.83	0.999	4×10^{13}	130.32	0.998
		10	4×10^{8}	75.58	0.999	7×10^{16}	168.65	0.997
		12	9×10^{8}	79.99	0.949	9×10^{28}	306.93	0.935
Vochysia ferruginea	0	0	9×10^{10}	93.16	0.998	3×10^{26}	225.20	0.901
	200	8	6×10^{8}	71.85	0.996	7×10^{11}	104.78	1.000
		10	6×10^{9}	81.67	0.999	2×10^{9}	78.04	0.999
		12	4×10^{8}	69.73	0.971	4×10^{24}	244.37	0.996
	225	8	4×10^{10}	88.96	0.999	1×10^{9}	71.99	0.995
		10	5×10^{9}	80.92	0.999	1×10^{30}	303.55	0.985
		12	3×10^{7}	63.22	0.998	1×10^{20}	198.03	0.993
	250	8	2×10^{11}	83.23	0.997	1×10^{13}	105.55	0.990
		10	1×10^{8}	68.60	1.000	1×10^{27}	274.73	0.981
		12	2×10^{6}	53.10	0.999	1×10^{36}	376.89	0.958

3.2. Devolatilization

Figure 4 displays the devolatilization rate of the torrefied and untorrefied biomasses. Table 5 shows when D_{max} was reached and the D_{max} values. For the *C. lusitanica* biomass, torrefaction at 250-10 and 250-12 had lower D_{rate} values (Figure 5a) and reached D_{max} more quickly (Table 5), whereas D_{max} increased between 200-8 and 225-12, and then decreased in biomass torrefied at 250 °C.

The *D. panamensis* biomass torrefied at 250 °C at the three temperatures had the lowest devolatilization rate. In addition, the shoulder in the devolatilization curve at 13 min disappeared in the biomass torrefied at 250 °C (Figure 4b). The time to reach D_{max} showed no significant variation, except for condition 250-12 where the time required was shorter and D_{max} increased with T_T and t_T, except for condition 250-12, where again the value was low (Table 5). *G. arborea* had the lowest devolatilization rate for all torrefactions, and especially for 225-10, 225-12, and 250 °C in the three t_T (Figure 4c). The time to reach D_{max} was approximately 16 min in the different types of biomass. However, the shortest time was obtained with 250-10 (Table 5). The D_{max} value increased at 225 °C, but decreased at 250 °C.

Table 5. Time to reach the maximum devolatilization rate determined by thermogravimetric analysis (TGA) experiments of the biomasses of five fast-growth plantation species in Costa Rica torrefied at different times and temperatures.

Species	Temperature (°C)	Time (min)	Time Max. (min)	D_{max} (% wt/min)
Cupressus lusitanica	0	0	18.33	17.3
	200	8	18.7	14.7
		10	18.8	14.1
		12	18.7	14.8
	225	8	18.6	16.1
		10	18.3	19.2
		12	18.3	18.8
	250	8	18.3	18.4
		10	17.0	8.2
		12	17.6	15.1
Dipteryx panamensis	0	0	18.0	18.6
	200	8	18.3	18.0
		10	18.3	18.2
		12	18.3	19.5
	225	8	18.3	20.7
		10	18.3	20.7
		12	18.2	21.1
	250	8	18.0	22.7
		10	18.0	20.5
		12	17.8	16.1
Gmelina arborea	0	0	16.7	16.9
	200	8	17.0	16.6
		10	16.8	14.5
		12	16.5	17.3
	225	8	16.6	17.9
		10	16.4	20.2
		12	16.6	14.0
	250	8	16.5	18.1
		10	14.4	13.7
		12	16.6	8.4

Table 5. *Cont.*

Species	Temperature (°C)	Time (min)	Time Max. (min)	D_{max} (% wt/min)
Tectona grandis	0	0	17.7	15.8
	200	8	17.9	14.6
		10	17.9	15.0
		12	17.7	15.8
	225	8	18.2	19.6
		10	18.1	19.3
		12	18.0	20.1
	250	8	18.1	20.2
		10	18.0	21.8
		12	17.6	16.5
Vochysia ferruginea	0	0	16.5	14.5
	200	8	17.0	15.7
		10	17.1	14.8
		12	16.4	16.2
	225	8	16.4	14.5
		10	16.4	16.6
		12	16.8	16.4
	250	8	17.0	17.3
		10	16.6	16.9
		12	16.4	17.9

The *T. grandis* torrefied biomass had a D_{rate} above 20 dw/dt, whereas torrefactions at 250-10 and 250-12 displayed no inflexion at 13 min (Figure 3d). The maximum devolatilization was reached at 17 min for the untorrefied biomass and 200 °C and 250-12 for torrefied biomass. Under other torrefaction conditions, the time exceeded 18 min. D_{max} increased with increasing T_T and t_T of torrefaction, with the exception of 250-12, which had a low D_{max} value (Table 5).

Under conditions 200-8, 200-10, and 225-8, the torrefied *V. ferruginea* had a lower D_{rate} relative to the torrefied and untorrefied biomass under the other conditions (Figure 4e). The time to reach D_{max} was close to 17 min, with a slight increase in the value of D_{max} with increasing T_T and t_T of torrefaction (Table 5).

Notably, in all species, once D_{max} was reached, the slope of the curve became more severe, with a steeper slope (Figure 4a–e).

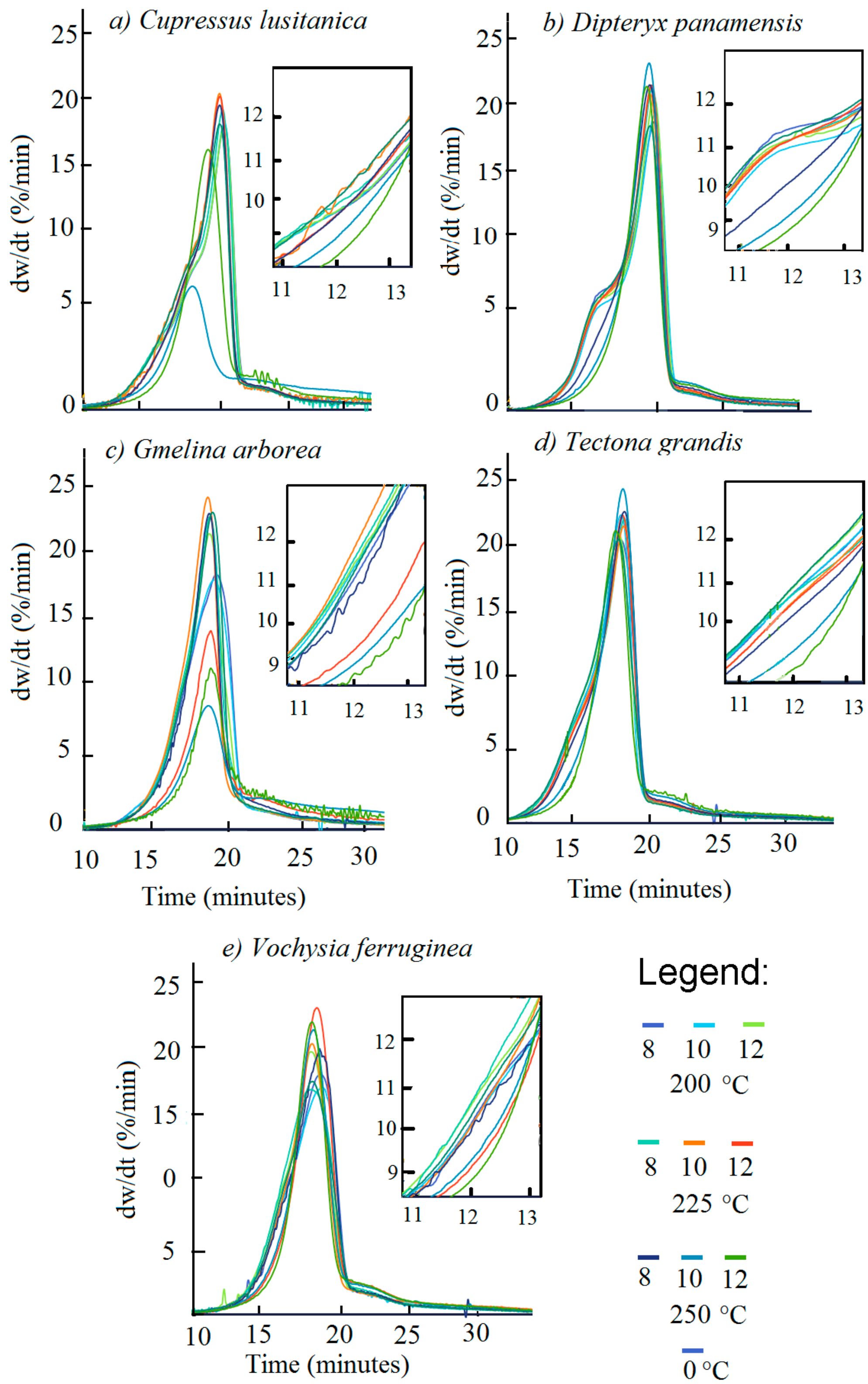

Figure 4. Devolatilization rate measured by the first derivative of the mass fraction with respect to time for the biomasses of for *Cupressus lusitanica* (**a**), *Dipteryx panamensis* (**b**), *Gmelina arborea* (**c**) and *Tectona grandis* (**d**) and *Vochysia guatemalensis* (**e**), torrefied at different times and temperatures.

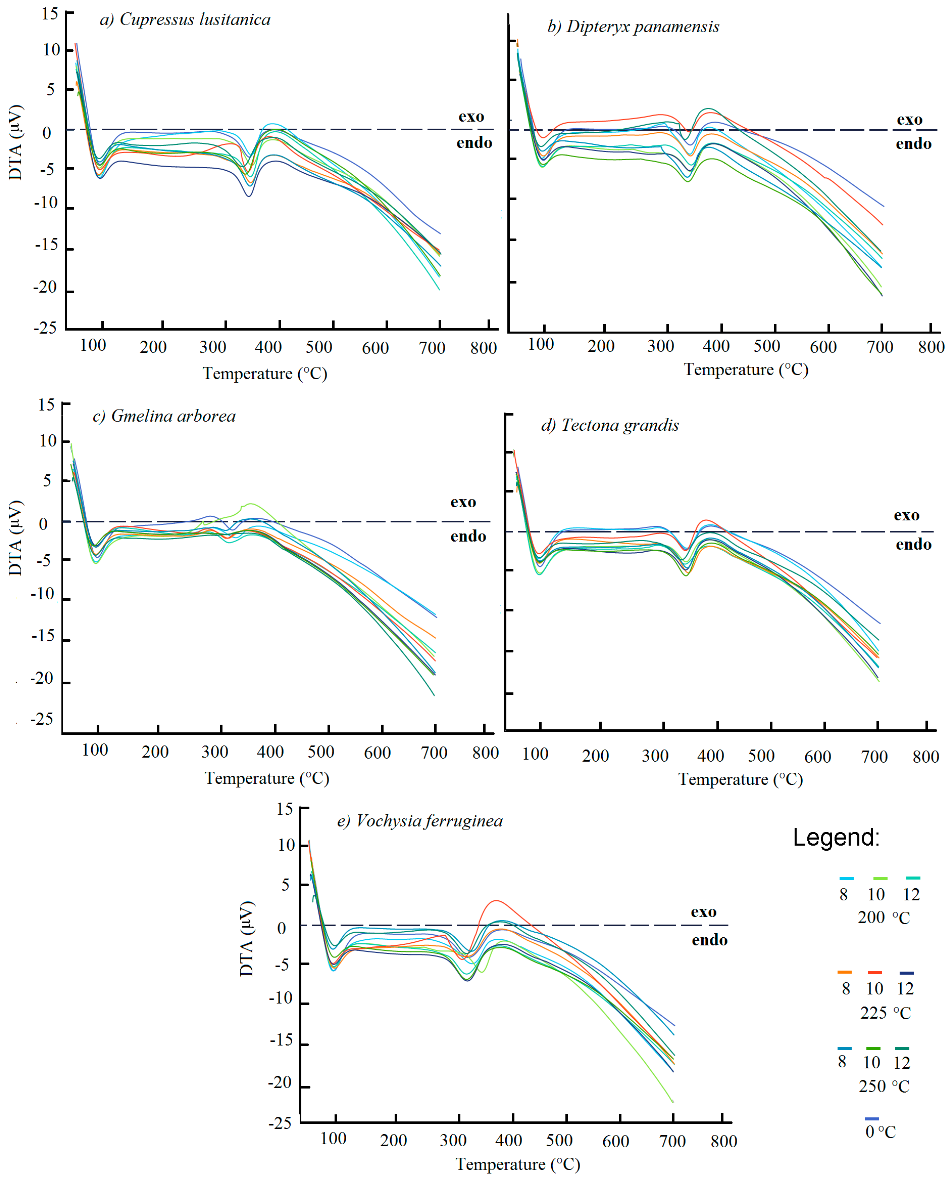

Figure 5. Differential Scanning Calorimetry (DSC) analysis of the torrefaction at different times and temperatures for for *Cupressus lusitanica* (**a**), *Dipteryx panamensis* (**b**), *Gmelina arborea* (**c**), *Tectona grandis* (**d**) and *Vochysia guatemalensis* (**e**).

3.3. Differential Scanning Calorimetry Analyses

Figure 5 displays the DTG curves of the calorimetric analysis of the reactions that occurred during the TGA. In all torrefaction conditions and for all woody species, the first endothermic peaks occurred at 100 and 300 °C, whereas exothermic peaks were observed between 350 and 400 °C, with some variations among the species and torrefaction conditions. All torrefaction conditions demonstrated endothermic processes in the *C. lusitanica* biomass. However, untorrefied biomass for condition 200-8 had a more pronounced exothermic peak between 350 and 450 °C (Figure 5a). In the *D. panamensis* biomass, torrefaction at 200-8, 200-12, 225-8, and 250-12 demonstrated exothermic processes between 350 and 450 °C, whereas endothermic peaks of greater magnitude were observed in biomass torrefied at 225-12, 250-10, and 250-12 (Figure 5c). Exothermic reactions occurred between 300 and 400 °C in *G. arborea* untorrefied biomass and with torrefaction at 200-8 and 225-10, whereas the biomass under the other torrefaction conditions only showed endothermic reactions (Figure 4c). For the *T. grandis* biomass, the exothermic reactions between 350 and 450 °C appeared in untorrefied biomass and under conditions 200-8 and 225-10 (Figure 5d). The opposite occurred in the biomass of *V. ferruginea*, as torrefied biomass presented exothermic peaks under severe torrefaction conditions (225-10, 250-10, and 250-12) (Figure 6e).

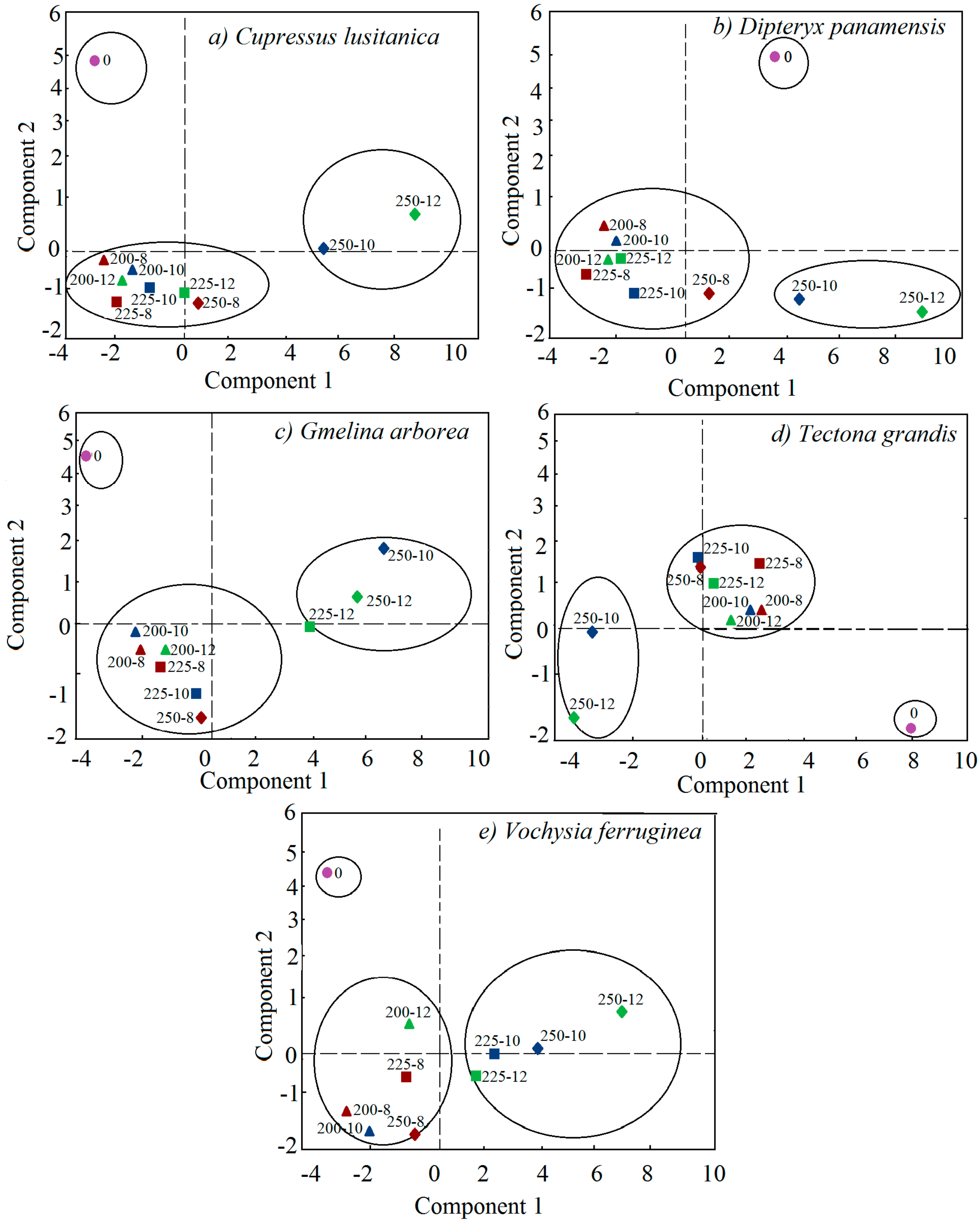

Figure 6. Relationship between the auto-vector of components 1 and 2 of the multivariate analysis by means of principal components of for *Cupressus lusitanica* (**a**), *Dipteryx panamensis* (**b**), *Gmelina arborea* (**c**) and *Tectona grandis* (**d**) and *Vochysia guatemalensis* (**e**), torrefied at different times and temperatures of five fast-growth plantations in Costa Rica.

3.4. Multivariate Analysis

Table 6 shows the MAPC that determined that the first two components represented approximately 60% of the total variation in the evaluated variables, of which 45% was explained by principle component one (PC1). In general, the variables influencing these components are related to hemicellulose for PC1, and cellulose for PC2. However, a slight variation was found between the different species (Table 6). For *C. lusitanica*, PC1 mainly included the hemicellulose-related variables, such as $T_{onset(hc)}$, $T_{offset(hc)}$, $W_{Tonset(hc)}$, $W_{Toffset(hc)}$, T_{sh}, and W_{Tsh}, and PC2 included cellulose variables such as $T_{onset(c)}$, $T_{offset(c)}$, and $W_{Tonset(c)}$. For *D. panamensis*, the variables that most influenced PC1 were the same as for *C. lusitanica* long with the Ea of hemicellulose and cellulose. In PC2, $T_{offset(c)}$, T_i, T_f, $W_{Toffset(c)}$, and W_{Ti} were the most influential. For *G. arborea*, the variables representing PC1 were percentage of residual mass, W_{Ti}, W_{Tm}, and W_{Tf}, whereas PC2 included $W_{Tonset(hc)}$, $W_{Tonset(c)}$, and W_{Ti}. The components of *T. grandis* included T_{sh}, T_i, mass residual, W_{Tsh}, $W_{Tm,}$ and W_{Tf} for PC1 and by $T_{onset(hc)}$, $T_{offset(hc)}$, T_{sh}, and $W_{Tonset(c)}$ for PC2. In *V. ferruginea*, PC1 included the percentage of residual mass, $W_{Tonset(hc)}$, $W_{Toffset(c)}$, W_{Ti}, W_{Tm}, and W_{Tf}, and PC2 included $T_{offset(hc)}$, $T_{onset(c)}$, T_i, and $W_{Tonset(c)}$.

By plotting the auto-vector for PC1 and PC2 for each species (Figure 6), we identified three different groups. In *C. lusitanica*, *D. panamensis* and *T. grandis*, the first group included torrefactions under 200 °C, 225 °C, and 250-8 °C; the second group included conditions 250-10 and 250-12; whereas the untorrefied biomass behaved differently compared with the other groups (Figure 5a–d). In *G. arborea*, the first group included torrefactions under 200 °C, 225-8, 225-10, and 250-8, whereas the second group included 225-12, 250-10, and 250-12. Similarly, the untorrefied biomass behaved differently compared with the other torrefactions (Figure 5c). The first *V. ferruginea* group was formed by torrefactions under 200 °C, 225-8, and 250-8; whereas the second group included 225-10, 225-50, 250-10, and 250-12. Untorrefied biomass had no similarities to any of the torrefactions (Figure 6e).

Table 6. Matrix of the multivariate analysis correlations for all variables evaluated of biomass torrefied at different times and temperatures of five fast-growth plantations species in Costa Rica.

Variable	*Cupressus Lusitanica*		*Dipteryx panamensis*		*Gmelina arborea*		*Tectona grandis*		*Vochysia ferruginea*	
	C1	**C2**	**C1**	**C2**	**C1**	**C2**	**C1**	**C2**	**C1**	**C2**
T_i (°C)	-	-	-	−0.92 **	-	-	−0.83 **	-	-	−0.80 **
T_m (°C)	−0.90 **	-	−0.89 *	-	-	-	-	-	-	-
T_f (°C)	-	-	-	0.79 **	-	-	-	−0.71 *	-	-
T_{sh} (°C)	−0.91 **	-	−0.78 **	-	-	-	0.83 **	-	-	-
$T_{offset(hc)}$ (°C)	−0.96 **	-	−0.69 **	−0.69 *	-	-	-	0.94 **	-	−0.93 **
$T_{onset(c)}$ (°C)	-	−0.97 **	−0.78 **	-	-	−0.87 **	-	0.88 **	-	−0.94 **
$T_{offset(c)}$ (°C)	-	0.89 **	-	0.97 **	-	-	-	−0.78 **	−0.69 *	-
$T_{onset(hc)}$ (°C)	0.97 **	-	0.95 **	-	-	-	-	−0.69 *	-	-
WT_{sh} (%)	0.97 **	-	-	-	-	-	−0.91 **	-	0.76 *	-
WT_i (%)	0.81 *	-	-	−0.87 **	-	−0.70 *	-	-	0.96 **	-
WT_m (%)	0.98 **	-	0.85 **	-	0.87 **	-	−0.96 **	-	0.87 **	-
WT_f (%)	0.98 **	-	0.80 **	-	0.96 **	-	−0.98 **	-	0.91 **	-
$WT_{onset(hc)}$ (%)	0.69 *	-	-	−0.85 **	-	−0.76 *	−0.66 *	0.71 *	0.78 **	-
$WT_{offset(hc)}$ (%)	0.97 **	-	0.91 **	-	0.93 **	-	−0.93 **	-	0.68 *	-
$WT_{onset(c)}$ (%)	-	0.79 *	0.96 **	-	-	0.79 *	-	−0.88 *	-	0.74 *
$WT_{offset\ (c)}$ (%)	0.96 **	-	0.75 *	−0.64 *	0.96 **	-	−0.98 **	-	0.94 **	-
Ea Hemicellulose	−0.72 *	-	−0.92 **	-	−0.93 **	-	-	0.75 *	−0.73 *	-
Ea Cellulose	0.73 *	-	0.86 **	-	0.69 *	-	−0.74 *	-	0.75 *	-
Residual mass (%)	0.98 **	-	0.80 *		0.96 **	-	−0.98 **	-	0.91 **	-
Time max (min)	−0.77 *	-	−0.95 **	-	−0.64 *	-	-	0.74 *	-	-
Rate max (wt/%)	-	-	-	-	−0.83 **	-	-	-	0.79 *	-
Percentage of variance	60.88	16.46	52.18	31.49	44.52	18.28	46.36	46.36	47.45	47.45
Cumulative variance	60.88	77.35	52.18	83.67	44.52	62.80	32.63	78.99	26.66	74.11

Note: C1: correlations of component 1; C2: correlations of component 2. * Significance at 95%, ** significance at 99%, - not present significance.

4. Discussion

4.1. TGA-DTG Analysis

In general, TGA trends for torrefied and untorrefied biomass of the different woody species were similar, which is consistent with previous reports [18,20,21]. The DTG curves support this finding, where important stages were defined (Figure 3a–e) and differences were clarified.

During thermogravimetric analyses, the initial decrease in mass is attributed to the release of the moisture in the samples [28]. This water release is lower for biomasses torrefied under more severe conditions, consistent with a higher drying temperature and an increase in the hydrophobicity related to such conditions [12]. Higher temperatures enable the decomposition of the polymers present in the samples. Hemicellulose degradation occurs between 230 and 330 °C [29]. This degradation mainly tends to disappear under severe torrefaction conditions for all five species because a higher percentage of hemicellulose has already been eliminated during torrefaction [4,28,30,31]. Then, cellulose decomposition occurs at temperatures between 305 and 380 °C [28,32], which appears in all the biomasses analyzed considering that torrefaction processes affect this biopolymer less than hemicellulose. Temperatures between 400 and 500 °C cause the final decomposition of cellulose and most of the lignin [33]. During this stage, the decomposition rate slows and then continues to a period of limited change as temperature increases.

The torrefied biomass displays the four decomposition stages of the well-defined components (Figure 3a–e). The first signal in the DTG curves before 150 °C is attributable to the removal of moisture in the samples, since moisture decreases with T_T [12]. The next signal or decomposition stage between 230 and 330 °C is due to hemicellulose degradation [29]; however, contrary to the untorrefied biomass, this signal tends to disappear under severe torrefaction in all five species (Figure 3). This is because high percentages of hemicelluloses have already been eliminated in the process prior to torrefaction [28,30]. This result agrees with the work reported by Bach et al. [31] and Ren et al. [4], who torrefied the biomass of conifers under temperatures above 250 °C and found that the signal decreased in the TGA curve. The next peak in the curve is related to cellulose decomposition, which occurs in the range of 305 to 380 °C [28,32]. This curve occurs in all torrefaction conditions and in untorrefied biomass, with differences in the magnitude of the peak, evidenced by weight loss. Lastly, in the final stage between 400 and 500 °C, the rate of decomposition slows, which is attributable to the final decomposition of cellulose and most of the lignin [33].

Using the parameters for material degradation (T_i, W_i) and hemicellulose degration ($T_{onset(hc)}$, $W_{Tonset\ (hc)}$), T_{sh}, $T_{offset(hc)}$), and $W_{Toffset(hc)}$)), the evaluation of stages two and three of the TGA curve shows that an increase of T_T and t_T increase T_i (Tables 2 and 3), indicating that torrefied biomass is more thermally stable than untorrefied biomass, which agrees with results found by Lee et al. [34] and Islam et al. [35] when evaluation some tropical species (*Dyera costulata*, *Esdospermun diadenum*, *Paraserianthes moluccana*, *Hevea brasiliensis*, and *Alstonia pneumatophora*). This result also indicates that an increase in T_T and t_T stabilizes the biomass, leading to a reduction in the mass loss values ($W_{Tonset(hc)}$ and $W_{Toffset(hc)}$) of this component (Table 4). Nevertheless, this behaviour should be viewed cautiously, as some authors indicated that this relationship is the result of the content of extractives in the wood, and the volatile material [27], affecting the combustion process [36]. In fact, Gaitán-Alvarez et al. [12] showed that, with these same woody species, weight loss during torrefaction is correlated with the type and content of extractives.

As for the cellulose degradation parameters, the evaluation showed that the most important differences were in temperature and residual mass at different T_T and t_T (Tables 2 and 3). The temperature parameters ($T_{onset(c)}$, T_m, and $T_{offset(c)}$) increased as T_T and t_T increased, except in *G. arborea* (Table 2), again indicating that this biomass component has higher thermal stability than in torrefied biomass, causing a reduction in weight loss values in the different stages of the evaluated cellulose decomposition evaluated ($W_{Tonset(c)}$, W_{Tm}, and $W_{Toffset(c)}$).

Some of the differences found in the species, or in the behaviour of the parameters evaluated in the decomposition of cellulose in torrefied biomass between species (Tables 2 and 3), show that the decomposition process of cellulose is complex in both torrefied and untorrefied biomass. The thermal stability of cellulose is related to the natural variation in the material, having a more chemically complex structure than hemicellulose [32,37]. Therefore, the parameters evaluated in the five species differ among them, even under the torrefaction conditions (Tables 3 and 4).

The activation energy was expected to increase with increasing T_T [38]. However, each structural component of the biomass has its own behaviour due to its chemical nature [39]. In the first stage, early degradation of hemicellulose appears during the torrefaction process [39]. Here, low activation energy is required to initiate hemicellulose degradation compared to activation energy of cellulose [38]. Hemicellulose starts to decompose at low temperatures, between 180 and 350°C [40]. Ramos [41] indicated that xylan, a type of hemicellulose, depolymerizes and reduces hemicelluloses into smaller molecules with lower molecular weight, which are more sensitive to pyrolysis [42]. Thus, with an increase in the torrefaction conditions in T_T and t_T, the hemicellulose decomposes in monosaccharides and volatilizes more rapidly [42]. For this reason, torrefied biomass has a low percentage of hemicellulose. Within the same woody species, Gaitán-Alvarez et al. [12] found that the weight loss of hemicellulose increases with T_T and t_T. Then, given the low hemicellulose content in the biomass torrefied under severe conditions, the activation energy is lower as T_T and t_T increase (Table 3). This result coincides with the studies of Bach et al. [43] on Norway spruce, Bobleter [44] on plants, and Wyman et al. [45] on biomass. These authors found that an increase in T_T significantly decreases the Ea in hemicellulose.

Cellulose degradation requires higher energy [38]. Biomass torrefaction increases the Ea value for cellulose (Table 4), since the thermal process increases the order of the regions of cellulose [40]. This means that heat transportation is more difficult [46], so the thermal stability of the biomass is greater [38]. This behaviour was observed in the biomasses studied, where the Ea for cellulose increased with increasing T_T and t_T, particularly under severe torrefaction conditions (Table 4).

4.2. Devolatilization

D_{max} is associated with the activation energy of cellulose decomposition. Higher Ea makes the polymer decomposition process more difficult, which is reflected in the lower D_{max} values and vice versa (Tables 4 and 5). Likewise, the decrease in devolatilization rates at higher temperatures at 250-10 and 250-12 (Figure 4a–e, Table 5) is attributed to the fact that at these T_T, a high proportion of hemicellulose has been degraded [27,46], leaving a low percentage of hemicellulose and less cellulose to devolatilize when the biomass is used for energy production. Likewise, a reduction in the devolatilization rate at the higher temperatures of 250-10 and 250-12 (Figure 4a–e, Table 5) is attributed to the degradation of a high proportion of hemicellulose at these T_T [27,46], leaving a low percentage of hemicellulose and less cellulose for devolatilization when the biomass is used for energy production.

The differences found in the devolatilization and D_{max} values among the various species (Figure 4a–e, Table 5) are associated with the proportion and nature of the hemicellulose and cellulose contained in the biomass, since each species has its unique behaviour and chemical structure, and therefore its own pyrolysis characteristics [18].

Chen et al. [5] showed that an increase in T_T and t_T affects D_{max}, without affecting the time to reach maximum devolatilization, with differences of approximately 2 min (Table 5). This behaviour indicates that, in torrefied biomass, the decomposition of cellulose (the component associated with maximum devolatilization) and the time to reach maximum devolatilization are maintained, whereas thermal stability of the torrefied biomass causes values of D_{max} to vary.

4.3. Differential Scanning Calorimetry Analyses

At temperatures below 200 °C, all DSC curves of the five species show endothermic values, which is linked to the energy biomass needs to absorb to remove moisture [32]. Later, the exothermic peaks at 275 °C correspond to degradation of hemicellulose, while yhe peak at 365 °C corresponds to ligninn [32,47]. The endothermic peak close to 355 °C corresponds to degradation of cellulose [32]. Figure 4a–e clearly shows the processes previously described.

Although all torrefied biomasses of the different species display the exothermic processes of hemicellulose and lignin and the endothermic process of cellulose [48,49], the different behavior of each species with respect to torrefaction conditions are evident. For the torrefied biomass of *C. lusitanica* (Figure 4a), the endothermic peaks at 375 °C are more pronounced than for the other species, indicating the greater stability of the cellulose in this species [38]. Conversely, in the torrefied biomass of *D. panamensis* and *T. grandis* (Figure 5b,d), the endothermic peaks at 375 °C are small or less pronounced, occurring mainly in the torrefaction conditions above 225-12, meaning that under these torrefaction conditions, cellulose is less stable [38].

The exothermic peaks at 275 °C corresponding to hemicellulose [48,49], are less pronounced or absent in some torrefied biomasses (Figure 5a–e), and especially in the biomass of *G. arborea* under all torrefaction conditions (Figure 5c). In the remainder of the species, this behaviour mainly appears under torrefaction conditions above 225-10 (Figure 5a,b,d,e). This is because at those T_T, part of the hemicellulose was removed during the torrefaction process [5]. Therefore, the exothermic peak with severe torrefaction is unclear [35].

4.4. Multivariate Analysis

The variables related to hemicellulose ($T_{onset(hc)}$, $T_{offset(hc)}$, $W_{Tonset(hc)}$, $W_{Toffset(hc)}$, T_{sh}, and W_{Tsh}) form PC1, whereas PC2 is related to the cellulose parameters (Table 6). This demonstrates that the behaviour of torrefied biomass at different T_T and t_T can be classified relative to the content of these components. In addition, these two components reflect the thermal stability of the torrefied biomass, as these were statistically and significantly reflected in the principal components (Table 3). However, the relationships between the principal components and the hemicellulose or cellulose parameters may not always be significant under some torrefied biomass conditions, likely due to the nature and quantity of these components in the biomass [18,21].

The scores of the components of the different types of biomass under torrefaction conditions display the different T_T and t_T conditions of hemicellulose and cellulose (Figure 6a,e, respectively). *C. lusitanica*, *D. panamensis*, and *T. grandis*, likely due to greater thermal stability under severe torrefaction conditions (250-10 and 250-12), form a unique group, different from the group formed with biomasses torrefied under light and middle torrefaction, which have similar conditions amongst the two groups. The torrefied biomass of *G. arborea* and *V. ferruginea* of form a group with biomasses torrefied under these conditions, different from biomass torrefied at 200 and 225 °C probably due to lesser thermal stability under condition 225-10 [5,18,21]. Then, the group formed by the different types of biomass torrefied under light and middle conditions, at 200 and 225 °C, respectively, indicate that these are the appropriate torrefaction conditions for those species, since they have the most appropriate parameters for combustion, such as positive correlation with D_{max} thermal stability (Table 6).

5. Conclusions

Based on our results, we conclude that the best torrefaction temperatures and times for the tested species are 200 °C for 8, 10, and 12 min and 225 °C for 8, 10, and 12 min, classified as light and medium torrefaction. Under these conditions, optimum thermo-chemical degradation is achieved for using biomass as an energy source, without significantly affecting the chemical composition of the material. In all species, severe torrefaction at 250 °C produced important degradation of the material, especially hemicellulose and part of the cellulose. As such, we do not recommend the use of this temperature in the biomass torrefaction of tropical species. However, behaviour among species presents some differences *C. lusitanica*, *D. panamensis* and *T. grandis* showed higher thermal stability that *G. arborea* and *V. ferruginea*.

Acknowledgments: The author thank the Vicerrectoría de Investigacion y Extension of the Instituto Tecnologico de Costa Rica and the Comsejo Nacional de Rectores (CONARE) for their financial support.

Author Contributions: Ana Rodriguez-Zúñiga and Róger Moya conceived and designed the experiments; Ana Rodriguez-Zúñiga and Róger Moya performed the experiments; Johanna Gaitán-Álvarez and Allen Puente-Urbina analyzed the data; Ana Rodriguez-Zúñiga and Róger Moya contributed reagents/materials/analysis tools; Johanna Gaitán-Álvarez and Róger Moya wrote the paper.

Conflicts of Interest: The authors declare no conflict of interest.

References

1. Yue, Y.; Singh, H.; Singh, B.; Mani, S. Torrefaction of sorghum biomass to improve fuel properties. *Bioresour. Technol.* **2017**, *232*, 372–379. [CrossRef] [PubMed]
2. Puig-Arnavat, M.; Shang, L.; Sárossy, Z.; Ahrenfeldt, J.; Henriksen, U.B. From a single pellet press to a bench scale pellet mill—Pelletizing six different biomass feedstocks. *Fuel Process. Technol.* **2016**, *142*, 27–33. [CrossRef]
3. Eseltine, D.; Thanapal, S.S.; Annamalai, K.; Ranjan, D. Torrefaction of woody biomass (Juniper and Mesquite) using inert and non-inert gases. *Fuel* **2013**, *113*, 379–388. [CrossRef]
4. Ren, S.; Lei, H.; Wang, L.; Bu, Q.; Chen, S.; Wu, J. Thermal behaviour and kinetic study for woody biomass torrefaction and torrefied biomass pyrolysis by TGA. *Biosyst. Eng.* **2013**, *116*, 420–426. [CrossRef]
5. Chen, W.H.; Peng, J.; Bi, X.T. A state-of-the-art review of biomass torrefaction, densification and applications. *Renew. Sustain. Energy Rev.* **2015**, *44*, 847–866. [CrossRef]
6. Medic, D.; Darr, M.; Shah, A.; Potter, B.; Zimmerman, J. Effects of torrefaction process parameters on biomass feedstock upgrading. *Fuel* **2012**, *91*, 47–154. [CrossRef]
7. Wang, G.; Luo, Y.; Deng, J.; Kuang, J.; Zhang, Y. Pretreatment of biomass by torrefaction. *Chin. Sci. Bull.* **2011**, *56*, 1442–1448. [CrossRef]
8. Peng, J.H.; Bi, X.T.; Sokhansanj, S.; Lim, C.J. Torrefaction and densification of different species of softwood residues. *Fuel* **2013**, *111*, 411–421. [CrossRef]
9. Van der Stelt, M.J.C.; Gerhauser, H.; Kiel, J.H.A.; Ptasinski, K.J. Biomass upgrading by torrefaction for the production of biofuels: A review. *Biomass Bioenergy* **2011**, *35*, 3748–3762. [CrossRef]
10. Chew, J.J.; Doshi, V. Recent advances in biomass pretreatment–Torrefaction fundamentals and technology. *Renew. Sustain. Energy Rev.* **2011**, *15*, 4212–4222. [CrossRef]
11. Ciolkosz, D.; Wallace, R. A review of torrefaction for bioenergy feedstock production. *Biofuel Bioprod. Biorefin.* **2011**, *5*, 317–329. [CrossRef]
12. Gaitán-Álvarez, J.; Moya, R.; Rodríguez-Zúñiga, A.; Puente-Urbina, A. Characterization of torrefied biomass of five reforestation species (*Cupressus lusitanica*, *Dipteryx panamensis*, *Gmelina arborea*, *Tectona grandis* and *Vochysia ferruginea*) in Costa Rica. *Bioresources* **2017**, *12*, 7566–7589. [CrossRef]
13. Da Silva, C.M.S.; Carneiro, A.D.; Pereira, B.L.C.; Vital, B.R.; Alves, I.C.N.; de Magalhaes, M.A. Stability to thermal degradation and chemical composition of woody biomass subjected to the torrefaction process. *Eur. J. Wood Prod.* **2016**, *74*, 845–850. [CrossRef]
14. Korošec, R.C.; Lavrič, B.; Rep, G.; Pohleven, F.; Bukovec, P. Thermogravimetry as a possible tool for determining modification degree of thermally treated Norway spruce wood. *J. Therm. Anal. Calorim.* **2009**, *98*, 189. [CrossRef]
15. Aydemir, D.; Gunduz, G.; Altuntas, E.; Ertas, M.; Sahin, H.T.; Alma, M.H. Investigating changes in the chemical constituents and dimensional stability of heat-treated hornbeam and uludag fir wood. *BioResources* **2011**, *6*, 1308–1321.
16. Vassilev, S.V.; Baxter, D.; Andersen, L.K.; Vassileva, C.G. An overview of the chemical composition of biomass. *Fuel* **2010**, *89*, 913–933. [CrossRef]
17. Poudel, J.; Ohm, T.I.; Oh, S.C. A study on torrefaction of food waste. *Fuel* **2015**, *140*, 275–281. [CrossRef]
18. Moya, R.; Rodríguez-Zúñiga, A.; Puente-Urbina, A. Thermogravimetric and devolatilisation analysis for five plantation species: Effect of extractives, ash compositions, chemical compositions and energy parameters. *Thermochim. Acta* **2017**, *647*, 36–46. [CrossRef]
19. Gaitán-Álvarez, J.; Moya, R. Characteristics and properties of pellet fabricated with torrefaccioned biomass of *Gmelina arborea* and *Dipterix panamensis* at different time. *Revista Chapingo* **2016**, *23*, 325–337.

20. Tenorio, C.; Moya, R. Thermogravimetric characteristics, its relation with extractives and chemical properties and combustion characteristics of ten fast-growth species in Costa Rica. *Thermochim. Acta* **2013**, *563*, 12–21. [CrossRef]
21. Gaitán-Álvarez, J.; Moya, R.; Puente-Urbina, A.; Rodríguez-Zúñiga, A. Physical and compression properties of pellets manufactured with the biomass of five woody tropical species of Costa Rica torrefied at different temperatures and times. *Energies* **2017**, *10*, 1205. [CrossRef]
22. Aragón-Garita, S.; Moya, R.; Bond, B.; Valaert, J.; Tomazello Filho, M. Production and quality analysis of pellets manufactured from five potential energy crops in the Northern Region of Costa Rica. *Biomass Bioenergy* **2016**, *87*, 84–95. [CrossRef]
23. Tenorio, C.; Moya, R.; Tomazello Filho, M.; Valaert, J. Application of the X-ray densitometry in the evaluation of the quality and mechanical properties of biomass pellets. *Fuel Process. Technol.* **2015**, *132*, 62–73. [CrossRef]
24. Tenorio, C.; Moya, R.; Tomazello-Filho, M.; Valaert, J. Quality of pellets made from agricultural and forestry crops in Costa Rican tropical climates. *BioResources* **2014**, *9*, 482–498. [CrossRef]
25. Moya, R.; Rodriguez-Zuñiga, A.; Puente-Urbina, A.; Gaitan-Alvarez, J. Study of light, middle and severe torrefaction and effects of extractives and chemical compositions on torrefaction process by thermogravimetric analyses in five fast-growing plantation of Costa Rica. *Energy* **2018**, *149*, 152–160. [CrossRef]
26. Sbirrazzuoli, N.; Vyazovkin, S.; Mititelu, A.; Sladic, C.; Vincent, L. A Study of Epoxy-Amine Cure Kinetics by Combining Isoconversional Analysis with Temperature Modulated DSC and Dynamic Rheometry. *Macromol. Chem. Phys.* **2003**, *204*, 1815–1821. [CrossRef]
27. Grønli, M.G.; Várhegyi, G.; Di Blasi, C. Thermogravimetric analysis and devolatilization kinetics of wood. *Ind. Eng. Chem. Res.* **2002**, *41*, 4201–4208. [CrossRef]
28. Prins, M.J.; Ptasinski, K.J.; Janssen, F.J. Torrefaction of wood: Part 2. Analysis of products. *J. Anal. Appl. Pyrolysis* **2006**, *77*, 35–40. [CrossRef]
29. Arias, B.; Pevida, C.; Fermoso, J.; Plaza, M.G.; Rubiera, F.; Pis, J.J. Influence of torrefaction on the grindability and reactivity of woody biomass. *Fuel Process. Technol.* **2008**, *89*, 169–175. [CrossRef]
30. Ramiah, M.V. Thermogravimetric and differential thermal analysis of cellulose, hemicellulose, and lignin. *J. Appl. Polym. Sci.* **1970**, *14*, 1323–1337. [CrossRef]
31. Bach, Q.V.; Skreiberg, Ø. Upgrading biomass fuels via wet torrefaction: A review and comparison with dry torrefaction. *Renew. Sustain. Energy Rev.* **2016**, *54*, 665–677. [CrossRef]
32. Yang, H.; Yan, R.; Chen, H.; Lee, D.H.; Zheng, C. Characteristics of hemicellulose, cellulose and lignin pyrolysis. *Fuel* **2007**, *86*, 1781–1788. [CrossRef]
33. Avni, E.; Coughlin, R.W. Kinetic analysis of lignin pyrolysis using non-isothermal TGA data. *Thermochim. Acta* **1985**, *90*, 157–167. [CrossRef]
34. Lee, S.Y.; Kang, I.A.; Doh, G.H.; Kim, W.J.; Kim, J.S.; Yoon, H.G.; Wu, Q. Thermal, mechanical and morphological properties of polypropylene/clay/wood flour nanocomposites. *Express Polym. Lett.* **2008**, *2*, 78–87. [CrossRef]
35. Islam, M.S.; Hamdan, S.; Rahman, M.R.; Jusoh, I.; Ahmen, A.S. Dynamic Young's modulus, morphological, and thermal stability of 5 tropical light hardwoods modified by benzene diazonium salt treatment. *BioResources* **2011**, *6*, 737–750.
36. Arteaga-Pérez, L.E.; Grandón, H.; Flores, M.; Segura, C.; Kelley, S.S. Steam torrefaction of *Eucalyptus globulus* for producing black pellets: A pilot-scale experience. *Bioresour. Technol.* **2017**, *238*, 194–204. [CrossRef] [PubMed]
37. McKendry, P. Energy production from biomass (part 2): Conversion technologies. *Bioresour. Technol.* **2002**, *83*, 47–54. [CrossRef]
38. Doddapaneni, T.R.; Konttinen, J.; Hukka, T.I.; Moilanen, A. Influence of torrefaction pretreatment on the pyrolysis of Eucalyptus clone: A study on kinetics, reaction mechanism and heat flow. *Ind. Crops Prod.* **2016**, *92*, 244–254. [CrossRef]
39. Chen, W.H.; Kuo, P.C. Torrefaction and co-torrefaction characterization of hemicellulose, cellulose and lignin as well as torrefaction of some basic constituents in biomass. *Energy* **2011**, *36*, 803–811. [CrossRef]
40. Park, J.; Meng, J.; Lim, K.H.; Rojas, O.J.; Park, S. Transformation of lignocellulosic biomass during torrefaction. *J. Anal. Appl. Pyrolysis* **2013**, *100*, 199–206. [CrossRef]

41. Ramos, L.P. The chemistry involved in the steam treatment of lignocellulosic materials. *Quim. Nova* **2003**, *26*, 863–871. [CrossRef]
42. Biswas, A.K.; Umeki, K.; Yang, W.; Blasiak, W. Change of pyrolysis characteristics and structure of woody biomass due to steam explosion pretreatment. *Fuel Process. Technol.* **2011**, *92*, 1849–1854. [CrossRef]
43. Bach, Q.V.; Tran, K.Q.; Skreiberg, Ø.; Khalil, R.A.; Phan, A.N. Effects of wet torrefaction on reactivity and kinetics of wood under air combustion conditions. *Fuel* **2014**, *137*, 375–383. [CrossRef]
44. Bobleter, O. Hydrothermal degradation of polymers derived from plants. *Prog. Polym. Sci.* **1994**, *19*, 797–841. [CrossRef]
45. Wyman, C.E.; Decker, S.R.; Himmel, M.E.; Brady, J.W.; Skopec, C.E.; Viikari, L. Hydrolysis of cellulose and hemicellulose. *Polysaccharides* **2005**, *1*, 1023–1062.
46. Skreiberg, A.; Skreiberg, Ø.; Sandquist, J.; Sørum, L. TGA and macro-TGA characterisation of biomass fuels and fuel mixtures. *Fuel* **2011**, *90*, 2182–2197. [CrossRef]
47. Ball, R.; McIntosh, A.C.; Brindley, J. Feedback processes in cellulose thermal decomposition: Implications for fire-retarding strategies and treatments. *Combust. Theory Model.* **2004**, *8*, 281–291. [CrossRef]
48. Shen, J.; Igathinathane, C.; Yu, M.; Pothula, A.K. Biomass pyrolysis and combustion integral and differential reaction heats with temperatures using thermogravimetric analysis/differential scanning calorimetry. *Bioresour. Technol.* **2015**, *185*, 89–98. [CrossRef] [PubMed]
49. Stenseng, M.; Jensen, A.; Dam-Johansen, K. Investigation of biomass pyrolysis by thermogravimetric analysis and differential scanning calorimetry. *J. Anal. Appl. Pyrolysis* **2001**, *58*, 765–780. [CrossRef]